J. Phys.: Condens. Matter **12** (2000) 2691–2699. Printed in the UK PII: S0953-8984(00)10508-9

The effect of electron–phonon interaction in iron-doped III–V cubic semiconductors

D Colignon†, E Kartheuser† and Murielle Villeret‡

† Institut de Physique, Université de Liège, Liège, Belgium

‡ Department of Mathematics, City University, London EC1V 0HB, UK

Received 22 December 1999

Abstract. A theoretical study of optical absorption and emission measurements of Fe^{2+} as a substitutional impurity in InP and GaP is presented. A new interpretation of the low-temperature absorption spectrum is proposed based on a weak Jahn–Teller interaction between the electronic excited states and a local gap mode of Γ_5 symmetry. The model also includes the crystal potential, hybridization with the orbitals of the ligands of the host crystal, spin–orbit interaction and a weak dynamic Jahn–Teller coupling of the orbital ground state of Fe^{2+} with transverse acoustic phonons of Γ_3 symmetry. The theoretical model describes with good accuracy the measured positions and relative intensities of the spectral lines. In addition, the mass dependence of the local gap mode of Γ_5 symmetry reproduces the general features of the fine structures associated with the isotopic shifts of the zero-phonon line and the contribution to the isotopic shifts arising from the difference in zero-point energy between the initial and final states of the transition is evaluated.

1. Introduction

The study of transition metal impurities in III–V semiconductors is of great practical and fundamental interest. The presence of deep iron acceptors in these materials can influence strongly their electrical and optical properties and have an appreciable effect on the performance of devices based on these compounds. For example, iron doping can produce semi-insulating materials, such as InP:Fe, that are of interest as high-resistivity substrates for epitaxial devices. The unintentional inclusion of iron in III–V compounds is also known to reduce the efficiency of light-emitting diodes and a detailed knowledge of the spectroscopic characteristics of iron in III–V materials is, therefore, highly desirable.

It is by now well known [1] that the iron impurity enters the lattice substitutionally, occupying random cation sites. Different charge states of iron occur in III–V semiconductors [1, 2]. In addition to the neutral Fe^{3+} ($3d^5$) state, the presence of the one-electron trap state Fe^{2+} ($3d^6$) has been detected, as well as, on occasions, the Fe^{+} ($3d^7$) state. Often, the Fe^{2+} state is dominant and gives rise to internal transitions within the d shell of the impurity that are observable with luminescence or optical absorption techniques. This was first demonstrated by Koschel *et al* [1] who observed, in the photoluminescence spectrum of InP:Fe, four well resolved zero-phonon lines with energies and intensities in agreement with transitions between spin–orbit-split levels of Fe^{2+} in a crystal field of T_d symmetry.

Similar conclusions were obtained by West *et al* [3] who performed detailed piezo-spectroscopic and Zeeman studies of the photoluminescence of GaP:Fe. Again four zero-phonon lines were observed that were attributed to transitions between crystal-field states of Fe^{2+} in sites with T_d symmetry. More importantly, these authors noted for the first time

0953-8984/00/122691+09$30.00

that crystal-field theory did not quite predict the energy splittings of the Fe^{2+} levels to within experimental error. They indicated that this may be due to the presence of a weak Jahn–Teller (JT) coupling with a phonon of low energy and made a crude estimate of the strength of the coupling. Subsequently, the existence of four zero-phonon lines was confirmed by Leyral *et al* [2, 4] for Fe^{2+} in InP and GaAs and by Shanabrook [5] for Fe^{2+} in GaP.

In the 1990s, the availability of high-purity samples with controlled concentrations of impurities and the development of high-resolution Fourier transform infrared spectrometers led to a revival of interest in the problem of Fe-doped III–V compounds [6–9]. Much more detailed studies of the optical absorption spectra of Fe-doped III–V materials were performed and additional lines linked to internal transitions of the Fe^{2+} levels were observed. In addition a fine structure originating from different iron isotopes has also been resolved [9].

A consequence of the more detailed experimental data is that it became clear that pure crystal-field theory cannot fully explain the spacings of zero-phonon lines and the isotopic fine structure. The existence of a Jahn–Teller coupling between the electronic states of the Fe^{2+} substitutional impurities and phonons or local vibrational modes of the host III–V semiconductor was investigated by a number of people [10–13]. All these papers focused on only some of the experimental data but did not attempt to explain with a single model the optical absorption, photoluminescence and isotopic measurements.

In this paper, we present a complete analysis of the emission and absorption spectra of InP:Fe^{2+} and GaP:Fe^{2+} using a coherent model that includes hybridization with the ligand orbitals, spin–orbit interaction and electron–phonon coupling. We propose a new interpretation of experimental data and show that the orbital excited states of Fe^{2+} couple with a local gap mode of Γ_5 symmetry. The inclusion of this mode in our calculation is essential for explaining the observed isotopic effect. In addition, we include a weak dynamic JT interaction between the electronic ground states and a transverse acoustic phonon of Γ_3 symmetry. We also evaluate the contribution to the isotopic shifts arising from the difference in zero-point energy between the initial and final states of the transition.

The paper is organized as follows. In section 2 we describe the theoretical model used to treat the electron–phonon interaction. Section 3 is devoted to a comparison of our results for the energies and intensities of the electric-dipole-allowed transitions with experiments. Finally, our conclusions are given in section 4.

2. Theoretical formalism

In semiconductors having the zinc-blende structure the magnetic ions are located at cation sites whose symmetry is tetrahedral (T_d). Within the framework of crystal-field theory, the ground term ^5D of the free Fe^{2+} ion separates into an orbital doublet $^5\Gamma_3$ and a triplet $^5\Gamma_5$, the former lying below the latter in energy [14]. The energy difference between these two orbital multiplets is denoted by Δ. The spin–orbit interaction further splits the tenfold-degenerate $^5\Gamma_3$ multiplet into five levels of symmetries Γ_1, Γ_4, Γ_3, Γ_5 and Γ_2, listed in order of increasing energy. The excited $^5\Gamma_5$ multiplet separates into levels of increasing energy Γ_5', Γ_4', Γ_3', Γ_5'', Γ_4'' and Γ_1' (see figure 1).

The effective electronic Hamiltonian for the ion is

$$H_{\text{ion}} = H_0 + V_c(T_d) + \lambda \boldsymbol{L}\cdot\boldsymbol{S} - \rho\left[(\boldsymbol{L}\cdot\boldsymbol{S})^2 + \frac{1}{2}\boldsymbol{L}\cdot\boldsymbol{S} - \frac{1}{3}L(L+1)S(S+1)\right] \tag{1}$$

where H_0 is the Hamiltonian of the free ion omitting the spin–orbit and spin–spin interactions [15] described respectively by the last two terms in equation (1) and the tetrahedral potential $V_c(T_d)$ leads to the separation Δ between the Γ_3 and Γ_5 multiplets [14]. Symmetry arguments

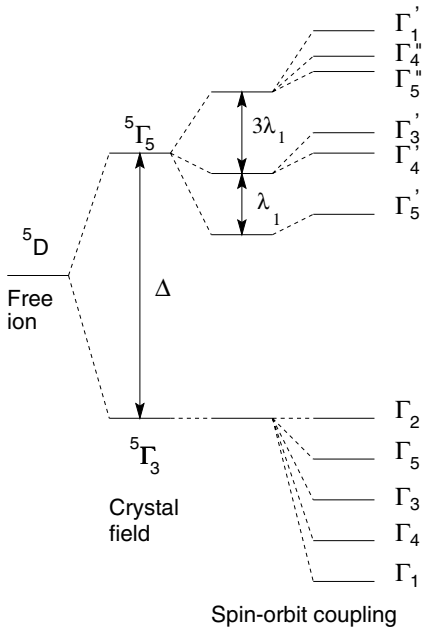

Figure 1. A schematic diagram of the energy levels of Fe^{2+} in a crystal field of tetrahedral symmetry (T_d) including the splittings due to the spin–orbit interaction.

show that there are, in principle, two different effective spin–orbit coupling constants: λ_1 corresponding to matrix elements within the Γ_5 orbital multiplet of the impurity and λ_2 for matrix elements mixing the Γ_5 and Γ_3 orbital states. They reflect the fact that the d electrons of the magnetic impurity at cation sites are not completely localized and spend part of their time in the vicinity of the anions. The electronic spin–orbit basis states are generated as products of wave functions involving orbital and spin parts. Figure 1 shows the symmetry of the twenty-five spin–orbit-split states of Fe^{2+}.

The theoretical formalism used to treat the dynamic JT coupling of the 3d electrons of the magnetic ion with vibrational modes of the crystal is similar to that described in reference [16]. This model has been applied successfully to the interpretation of the near-infrared absorption and emission data for doubly ionized iron in cubic II–VI semiconductors (CdTe, ZnTe, ZnSe and ZnS [17]). It is now extended to treat InP:Fe^{2+} and GaP:Fe^{2+}.

For the purpose of this investigation, the vibrational modes of the crystal are best classified according to the site symmetry of the magnetic ion rather than according to the space group of the host. From symmetry considerations, it follows that matrix elements of the JT interaction between states of the Γ_3 multiplet vanish for a phonon mode of symmetry Γ_5 but not for a phonon of symmetry Γ_3 while matrix elements connecting states in the Γ_5 multiplet need not vanish for phonons of symmetries Γ_3 and Γ_5. Therefore we write the phonon and electron–phonon coupling Hamiltonians as

$$H_{\mathrm{p}} = \hbar\omega_3 \sum_{i=1}^{2}\left(a_i^{\dagger}a_i + \frac{1}{2}\right) + \sum_{i=1}^{2}(a_i^{\dagger} + a_i)U_i^{(3)} + \hbar\omega_5 \sum_{j=1}^{3}\left(b_j^{\dagger}b_j + \frac{1}{2}\right) + \sum_{j=1}^{3}(b_j^{\dagger} + b_j)U_j^{(5)}. \tag{2}$$

Here a_i ($a_i^{\dagger}$) is a destruction (creation) operator for a phonon belonging to the ith row of Γ_3. A similar statement is applicable to b_j, where j labels the rows of Γ_5; $\hbar\omega_3$ and $\hbar\omega_5$ are the

energies of phonons of Γ_3 and Γ_5 symmetries, respectively. The 5×5 matrices $U_i^{(3)}$ and $U_j^{(5)}$ are electronic operators whose elements are given by group theoretical considerations [16] and are proportional to $E_{\mathrm{JT}}^{(3)}$ or $E_{\mathrm{JT}}^{(5)}$, the JT energies for the Γ_3 and Γ_5 phonons, respectively. The phonon states and their overtones are classified according to the irreducible representations of the group T_d and are listed in references [16, 18].

To find the eigenvalues of the total Hamiltonian operator ($H = H_{\mathrm{ion}} + H_{\mathrm{p}}$) we start from a set of symmetry-adapted wave functions which are linear combinations of electronic and vibrational states with coefficients given by the Clebsch–Gordan coefficients for the group T_d [19]. At this stage, it is worth noticing that, even though the Γ_5 phonons do not couple to the electronic Γ_3 states via H_{p}, it is necessary to include in our basis the vibronic states involving electronic levels in the Γ_3 manifold and phonons of Γ_5 symmetry. The reason for this is that the spin–orbit interaction between vibronic states originating from the Γ_3 and Γ_5 multiplets alters the spacing of the vibronic levels after modification by the JT interaction. However, a good approximation is obtained by restricting the basis to the states containing overtones of only one kind of vibrational mode at a time (Γ_3 or Γ_5). With the set of basis vectors obtained in this fashion, the Hamiltonian appears in blocks associated with the irreducible representations Γ_i ($i = 1, 2, \ldots, 5$) of T_d in the notation of Koster *et al* [19].

It will be shown in section 3 that, in the cases of InP:Fe^{2+} and GaP:Fe^{2+}, the optical measurements demonstrate clearly that there is a weak Jahn–Teller interaction between the excited orbital multiplet of Fe^{2+} and a local gap mode of symmetry Γ_5 in addition to a weak JT interaction between the orbital ground state of Fe^{2+} and a Γ_3 phonon of the host crystal.

3. Discussion and comparison between theory and experiment

A large number of theoretical [10–12] and experimental [6–9] investigations have been devoted to the study of the 2+ charge state of iron in III–V semiconductors such as InP, GaP and GaAs. In the present section we analyse the most recent high-resolution data of Pressel *et al* [7] on InP:Fe^{2+} and of Rückert *et al* [9] on GaP:Fe^{2+} in the framework of the theoretical model described in section 2. Most previous theoretical papers have focused on the interpretation of the emission spectrum related to electric-dipole transitions from the Γ_5' spin–orbit-split state (see figure 1) to the ground state Γ_1. However, very little consideration [11] has been given to the absorption measurements. The vibronic model presented in this paper accounts for both emission and absorption spectra and also reproduces the general features of the fine structure associated with the isotopic shifts of the zero-phonon line ($\Gamma_1 \leftrightarrow \Gamma_5'$ ($1 \leftrightarrow 5'$) transition).

We first discuss the case of InP:Fe^{2+} and look at the low-temperature absorption spectrum. At low temperature, the infrared spectrum consists mainly of three lines at 2843.9 (line I), 3117.0 (line II) and 3135.9 (line III) cm^{-1}. Lines I and III are very narrow, sharp lines while line II has a much larger full width at half-maximum (FWHM). In addition, line I exhibits a fine structure that has been attributed to the different isotopes of Fe^{2+} impurity. This line is the zero-phonon $\Gamma_1 \rightarrow \Gamma_5'$ transition but the interpretation of the other two lines is still open to conjecture.

In agreement with earlier work [16], we take as phonon mode interacting with the orbital ground state a transverse acoustic phonon (TA(L)) of Γ_3 symmetry and energy $\hbar\omega_3 = 55\ cm^{-1}$ [20]. In addition, in order to explain the low-temperature spectrum we introduce a JT interaction with a local gap mode of Γ_5 symmetry. The introduction of this mode is also essential to explain the observed isotopic shifts of the zero-phonon line (2843.9 cm^{-1}). Within this framework we propose an interpretation of the absorption spectra which differs from that of Pressel *et al* [7] in the attribution of the absorption lines at 3117 cm^{-1} and 3135.9 cm^{-1}. We assume that the first of these lines corresponds to a transition ($1 \rightarrow 5'a$) from the ground state Γ_1 to a vibronic

state involving the electronic Γ_5' state and the first overtone of the local gap mode and that the second line at 3135.9 cm^{-1} corresponds to the electronic transition $1 \rightarrow 5''$.

This new interpretation is supported by the different lineshapes of the two lines and their relative intensities. At low temperature, zero-phonon lines have very sharp, narrow lineshapes but transitions involving vibronic states tend to have broader FWHM. This confirms our assignment of lines I and III to zero-phonon lines and of line II to a transition involving vibronic states.

Before discussing the numerical calculations for the full spectrum (at any temperature), it is of interest to first investigate lines II and III with a simple analytical model that shows clearly the interrelationship between the energies of these lines, the JT energy and the gap mode energy. This is done by restricting the Hamiltonian basis to a subset of states containing only the two symmetry-adapted wave functions $|\epsilon''; A^{(5)}(0)\rangle$ and $|\epsilon'; E^{(5)}(1)\rangle$. These two states are the predominant contribution to the $5'$a and $5''$ levels. The notation used here is that of reference [16]. The states are products of electronic and vibrational states; ϵ' and ϵ'' are the electronic states Γ_5' and Γ_5'', $A^{(5)}(0)$ is the phonon vacuum state (of symmetry Γ_1) and $E^{(5)}(1)$ is the first overtone of the Γ_5 phonon, belonging to the irreducible representation Γ_3 (for details, see reference [16]). The zero of energy is taken at the Γ_1 ground state. The Hamiltonian matrix in this reduced basis is then given by

$$\begin{pmatrix} \Delta - 2\lambda_1 & \sqrt{6}K/5 \\ \sqrt{6}K/5 & \Delta + 3\lambda_1 + \hbar\omega_5 \end{pmatrix} \tag{3}$$

where K is related to the JT energy by $K^2 = \frac{3}{2}\hbar\omega_5 E_{JT}$. It should be mentioned that these two lines are resonant lines if the energy of the gap mode, $\hbar\omega_5$, is comparable to $-5\lambda_1$. The diagonalization of this matrix leads to the energies E_{II} and E_{III} of lines II and III. The expressions for E_{II} and E_{III} can then be used to obtain information on the dependence of E_{JT} on the gap mode energy, $\hbar\omega_5$. From the relationship between K and E_{JT} and the energy difference $\Delta E = E_{III} - E_{II}$ we finally obtain

$$E_{JT} = \frac{25}{36}\frac{(\Delta E)^2 - (5\lambda_1 + \hbar\omega_5)^2}{\hbar\omega_5}. \tag{4}$$

From the experimental data, we know that the energy difference between lines II and III is 18.9 cm^{-1}. Fixing ΔE at 18.9 cm^{-1} and taking approximate values $\Delta = 2950.0$ cm^{-1} and $\lambda_1 = -56.0$ cm^{-1} [21], we can now look at the evolution of E_{JT} as a function of the gap mode energy, $\hbar\omega_5$. This is displayed in figure 2(a). Moreover, from the eigenstates of the above

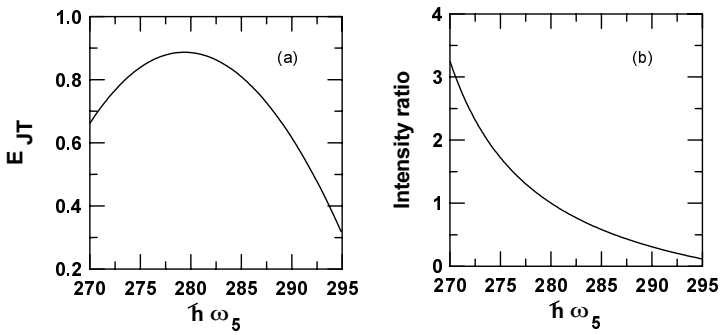

Figure 2. The evolution of (a) E_{JT} and (b) the intensity ratio as functions of the gap mode energy, $\hbar\omega_5$.

matrix, we can obtain the dependence of the intensity ratio of line III and to line II on $\hbar\omega_5$, i.e.,

$$I = \frac{9\hbar\omega_5 E_{\mathrm{JT}} + 25(\Delta - 2\lambda_1 - E_{\mathrm{III}})^2}{9\hbar\omega_5 E_{\mathrm{JT}} + 25(\Delta - 2\lambda_1 - E_{\mathrm{II}})^2}. \tag{5}$$

This is displayed in figure 2(b). These two figures can be used to get an idea of the approximate values of E_{JT} and $\hbar\omega_5$ that need to be used in the full numerical calculation. In order to explain the isotopic shifts of line I, it is most favourable to have as large a JT energy as possible [13]. At the same time, one must also reproduce the intensity ratio of line III to line II. As figure 2(b) shows, the intensity ratio decreases rapidly and from figure 2(a) it appears favourable to have $\hbar\omega_5$ close to 280 cm^{-1}. After making various fine-tuned adjustments to the parameters, this is indeed the value that we will adopt in the numerical calculations.

We are now in a position to discuss the exact numerical calculation and the fit to the complete spectrum (including spectral lines observed at higher temperature). Details of the vibronic basis are given in reference [16]. The Hamiltonian is first diagonalized using the starting values of the parameters mentioned in the previous discussion and the final values of the parameters are obtained by a self-consistent fitting procedure given in reference [16]. We note that to obtain convergence for the energies of the vibronic states it was necessary to include overtones up to order $n = 12$. The physical parameters obtained from the comparison between theory and experiment are listed in table 1. In the first column of table 1 we display our assignment of the transitions. The notation used to designate the energy levels of the system is as follows: we give their symmetry by the index $1, 2, \ldots, 5$ of the irreducible representation in the notation of Koster *et al* [19] and an alphabetical index which simply gives the order of increasing energy. The experimental and calculated values of the transition energies are listed in columns 2 and 3 of table 1, respectively. Finally, the last column gives the intensities of the electric-dipole-allowed transitions relative to that of the zero-phonon line ($1 \leftrightarrow 5'$). These values do not take into account the thermal population effects that have to be included for all transitions not originating from the ground state. At $T = 16$ K, the population factors are 0.3, 0.1 and 0.02 for transitions originating from Γ_4, Γ_3 and Γ_5, respectively. Finally, we point out

Table 1. Comparison between the calculated and experimental energies in InP:Fe^{2+}. The last column gives the calculated relative intensities, taking as unity the intensity of the reference line at 2843.9 cm^{-1}. Parameters: $\Delta = 2946.3\ \mathrm{cm}^{-1}$, $\lambda_1 = -56.4\ \mathrm{cm}^{-1}$, $\lambda_2 = -76.8\ \mathrm{cm}^{-1}$, $\rho = 0.95\,\mathrm{cm}^{-1}$, $\hbar\omega_3 = 55.0\,\mathrm{cm}^{-1}$, $E_{\mathrm{JT}}^{(3)} = 4.75\,\mathrm{cm}^{-1}$, $\hbar\omega_5 = 280.0\,\mathrm{cm}^{-1}$ and $E_{\mathrm{JT}}^{(5)} = 0.82\,\mathrm{cm}^{-1}$.

Transition	Experimental energy (cm^{-1})	Calculated energy (cm^{-1})	Relative intensity
$5 \rightarrow 5'$	2801.8	2802.5	0.90
$3 \rightarrow 5'$	2819.7	2818.9	1.00
$4 \rightarrow 5'$	2830.2	2830.2	2.00
$1 \rightarrow 5'$	2843.9	2843.9	1.00
$3 \rightarrow 4'$	2938.0	2841.5	1.23
$4 \rightarrow 4'$	2949.0	2952.8	1.37
$4 \rightarrow 3'$		2960.1	0.0002
$5 \rightarrow 5'$a	3074.0	3075.6	0.14
$3 \rightarrow 5'$a	3092.0	3092.0	0.44
$4 \rightarrow 5'$a	3103.3	3103.3	0.53
$4 \rightarrow 5'$b		3103.6	0.57
$1 \rightarrow 5'$a	3117.0	3117.0	0.54
$4 \rightarrow 5''$	3122.2	3122.2	1.00
$4 \rightarrow 4''$		3131.6	1.73
$1 \rightarrow 5''$	3135.9	3135.9	0.98

that the results of table 1 differ in one more respect from the interpretation of Pressel *et al* [7]. Pressel *et al* assign the $\Gamma_4 \rightarrow \Gamma_3'$ transition to a weak line observed in their spectrum at 2874 cm^{-1}. This interpretation requires that the Γ_3' state lie below the Γ_4' state, in contradiction with predictions of crystal-field theory. However, our calculation leads to an energy of 2960 cm^{-1} for the $\Gamma_4 \rightarrow \Gamma_3'$ transition but our evaluation of intensities predicts that this line is far too weak to be observed. In addition we found that the Γ_3' state always lies above the Γ_4' state in agreement with the conclusions of reference [11].

It is important to note that the energy of the local gap mode used to fit the absorption spectrum has been taken equal to $\hbar\omega_5 = 280$ cm^{-1}. This is lower than the energy (295 cm^{-1}) quoted by Pressel *et al* and obtained from the emission data. This change in energy can be related to the difference in the electronic charge distributions of the excited ($^5\Gamma_5$) and ground ($^5\Gamma_3$) orbital multiplets, respectively [22]. The frequencies 280 cm^{-1} and 295 cm^{-1} are those of the gap mode of the most abundant stable isotope of Fe (i.e., ^{56}Fe) in its excited and ground state, respectively. They depend on the isotopic mass of the Fe^{2+} impurity and will contribute to the isotopic shift of the zero-phonon line. To describe the mass dependence of the gap mode frequency we use the MX_4 molecular model [13, 23]. This model assumes a central atom of mass M (i.e., Fe) surrounded by a tetrahedral cage of nearest-neighbour cations of mass M_- (i.e., P). The vibrational modes of the MX_4 molecule are classified according to the irreducible representations of T_d as $\Gamma_1 + \Gamma_3 + 2\Gamma_5$ but, in the Γ_1 and Γ_3 mode, the central atom remains stationary while this is not the case for the Γ_5 modes whose frequencies depend on M. If bond bending is neglected, the frequency of one of the Γ_5 modes vanishes while that of the other Γ_5 mode is

$$\omega(\Gamma_5) = \left[\frac{k_r}{M_-}\left(1 + \frac{4M_-}{3M}\right)\right]^{1/2}. \tag{6}$$

Here k_r is the bond-stretching force constant. The values of k_r, obtained from the frequencies quoted above, are $k_r^g = 91.3$ N m^{-1} and $k_r^e = 82.2$ N m^{-1}, for the ground and excited states respectively. With these values of k_r one can the obtain the frequencies of the gap modes for the other stable isotopes of Fe. For example, for ^{54}Fe, we get $\hbar\omega_5 = 297.159$ cm^{-1} for the ground state and 281.961 cm^{-1} for the excited state.

With this information we can evaluate the two contributions to the isotopic shift of the zero-phonon line. The first contribution comes from the JT interaction and is obtained numerically. For InP:Fe^{2+}, with the parameters used in this paper, this leads to an isotopic shift between ^{56}Fe and ^{54}Fe of 0.015 cm^{-1}, much smaller than the observed isotopic shift of 0.31 cm^{-1}. However, there is also a contribution from the difference in zero-point energy between the initial and final states of the transition, due to the different electronic charge distributions in those electronic states, i.e., the different force constants k_r^g and k_r^e. For ^{56}Fe, the zero-point contribution to the energy of line I is $\frac{3}{2}(280 - 295) = -22.5$ cm^{-1} whereas for ^{54}Fe it is -22.797 cm^{-1}. This means that the zero-phonon transition for ^{54}Fe is shifted downwards by 0.297 cm^{-1} compared to the ^{56}Fe zero-phonon line.

A similar interpretation is applied to the case of GaP:Fe^{2+} and the results and parameters are shown in table 2. In this case again, the results are in good agreement with experiment except for one major discrepancy concerning the transitions $3 \rightarrow 4'$ and $4 \rightarrow 4'$. Our calculation predicts these transitions at energies 3452.0 cm^{-1} and 3463.3 cm^{-1} whereas the observed energies are 3405 and 3416 cm^{-1}, respectively. However, this discrepancy could be explained by the fact that, as mentioned by Rückert *et al* [9], this region of the spectrum is obscured by instabilities in the spectral characteristics of their spectrometer.

Finally, we comment on the values of the spin–orbit coupling constants λ_1 and λ_2. The magnitudes of these two constants both decrease compared to the free-ion value. The ratio

Table 2. Comparison between the calculated and experimental energies in GaP:Fe^{2+}. Parameters: $\Delta = 3458.27\ cm^{-1}$, $\lambda_1 = -62.1\ cm^{-1}$, $\lambda_2 = -80.3\ cm^{-1}$, $\rho = 0.95\ cm^{-1}$, $\hbar\omega_3 = 83.0\ cm^{-1}$, $E_{JT}^{(3)} = 9.0\ cm^{-1}$, $\hbar\omega_5 = 310.0\ cm^{-1}$, $E_{JT}^{(5)} = 0.76\ cm^{-1}$.

Transition	Experimental energy (cm^{-1})	Calculated energy (cm^{-1})	Relative intensity
$5 \rightarrow 5'$	3302.5	3303.0	0.60
$3 \rightarrow 5'$	3318.7	3318.2	0.86
$4 \rightarrow 5'$	3329.5	3329.5	2.06
$1 \rightarrow 5'$	3342.3	3342.3	1.00
$3 \rightarrow 4'$	3405.0	3452.0	1.35
$4 \rightarrow 4'$	3416.0	3463.3	1.36
$4 \rightarrow 3'$		3469.6	0.0001
$5 \rightarrow 5'a$	3605.0	3605.5	0.17
$3 \rightarrow 5'a$	3621.0	3620.7	0.54
$4 \rightarrow 5'a$	3632.0	3632.0	0.58
$4 \rightarrow 4'a$		3632.2	0.84
$1 \rightarrow 5'a$	3644.8	3644.8	0.59
$3 \rightarrow 5''$		3639.5	0.84
$4 \rightarrow 5''$		3650.8	0.96
$4 \rightarrow 4''$		3659.1	1.69
$1 \rightarrow 5''$	3663.6	3663.6	0.94

$\lambda_1/\lambda_{\text{free ion}} = 0.56$ (InP:Fe) and 0.62 (GaP:Fe) is much smaller than in the case of II–VI semiconductors [24]. This ratio is a measure of the degree of covalency of the Fe–P bonds and, following the theory of Vallin and Watkins [21], the ratio 0.56 (0.62) means that the d electrons of the Fe ion spend 56% (62%) of their time in the vicinity of the magnetic impurity and 44% (38%) of the time in the vicinity of the phosphorus atoms. The theory of Vallin and Watkins allows an analytic evaluation of λ_1 and λ_2 if one knows the values ζ_d and ζ_L of the one-electron spin–orbit coupling constants of the impurity and the ligands. In our case the Vallin and Watkins theory would predict

$$\lambda_1 = -0.205(\zeta_d - 0.51\zeta_L) = -56.4\ \text{cm}^{-1} \tag{7}$$

and

$$\lambda_2 = 0.2(\zeta_d - 0.06\zeta_L) = -77.0\ \text{cm}^{-1} \tag{8}$$

where we have used $\zeta_d = 400\ cm^{-1}$ and $\zeta_L = 245\ cm^{-1}$ [25]. The values of λ_1 and λ_2 obtained from our self-consistent fitting procedure are in excellent agreement with the values in equations (7) and (8).

4. Conclusions

We have shown that the vibronic model presented here accounts well for the absorption and emission spectra of InP:Fe^{2+} and GaP:Fe^{2+} if we take into account a weak dynamic Jahn–Teller coupling of the orbital excited state of the magnetic ion with a local gap mode of Γ_5 symmetry, in addition to the more commonly used interaction between the orbital ground state and transverse acoustic phonons of Γ_3 symmetry. The inclusion of the gap mode is vital for explaining the resonant absorption lines and the isotopic shifts of the zero-phonon line. We proposed a new interpretation of both the emission and absorption spectra of Fe^{2+} in InP and GaP, which also accounts for the isotopic shifts of the zero-phonon line observed in this compound. Finally, the spin–orbit coupling constants deduced from our calculations show that

the covalent character of the bonds is much more important in III–V compounds than in II–VI compounds such as ZnS [24].

Acknowledgments

This work was supported by the North Atlantic Treaty Organization (NATO Research Grant No 960666) and by the Fonds National de la Recherche Scientifique (Grant No 9.456.96F).

References

[1] Koschel W H, Kaufmann U and Bishop S G 1977 *Solid State Commun.* **21** 1069
[2] Leyral P, Brémond G, Nouailhat A and Guillot G 1981 *J. Lumin.* **24+25** 245
[3] West C L, Hayes W, Ryan J F and Dean P J 1980 *J. Phys. C: Solid State Phys.* **13** 5631
[4] Leyral P, Charreaux C and Guillot G 1988 *J. Lumin.* **40+41** 329
[5] Shanabrook B V, Klein P B and Bishop S G 1983 *Physica* B **116** 444
[6] Thonke K and Pressel K 1991 *Phys. Rev.* B **44** 13 418
[7] Pressel K, Thonke K, Dörnen A and Pensl G 1991 *Phys. Rev.* B **43** 2239
[8] Pressel K, Rückert G, Dörnen A and Thonke K 1992 *Phys. Rev.* B **46** 13 171
[9] Rückert G, Pressel K, Dörnen A, Thonke K and Ulrici W 1992 *Phys. Rev.* B **46** 13 207
[10] Vogel E E, Mualin O, de Orúe M A and Rivera-Iratchet J 1991 *Phys. Rev.* B **44** 1579
Vogel E E, Mualin O, de Orúe M A and Rivera-Iratchet J 1994 *Phys. Rev.* B **49** 2907
[11] Gavaix A M 1996 *J. Phys.: Condens. Matter* **8** 1163
[12] Kaufmann B and Dörnen A 1997 *Z. Phys. Chem.* **201** 111
[13] Colignon D, Mailleux E, Kartheuser E, Rodriguez S and Villeret M 1998 *Solid State Commun.* **105** 205
[14] Villeret M, Rodriguez S and Kartheuser E 1990 *Phys. Rev.* B **41** 10 028
[15] Abragam A and Bleaney B 1970 *Electron Paramagnetic Resonance of Transition Ions* (Oxford: Clarendon)
[16] Colignon D, Kartheuser E, Rodriguez S and Villeret M 1995 *Phys. Rev.* B **51** 4849
[17] Colignon D and Kartheuser E 1997 *Z. Phys. Chem.* **201** 119
[18] Savona V, Bassani F and Rodriguez S 1994 *Phys. Rev.* B **49** 2408
[19] The group theoretical notation for the point groups and the irreducible representations follows
Koster G F, Dimmock J O, Wheeler R G and Statz H 1966 *Properties of the Thirty-Two Point Groups* (Cambridge, MA: MIT press)
[20] Borcherds P H, Alfrey G F, Saunderson D H and Woods A D B 1975 *J. Phys. C: Solid State Phys.* **8** 2002
[21] Vallin J T and Watkins G D 1966 *Phys. Rev.* B **9** 2051
[22] Dahan P, Fleurov V, Thurian P, Heitz R, Hoffmann A and Broser I 1998 *Phys. Rev.* B **57** 9690
[23] See, for example,
Ballhausen C J 1962 *Introduction to Ligand Field Theory* (New York: McGraw-Hill)
Wadia W 1968 *Theor. Chim. Acta* **12** 104
[24] Colignon D, Mailleux E, Kartheuser E and Villeret M 1998 *Phys. Rev.* B **57** 12 932
[25] The value of ζ_L for P is taken from
Barnes R G and Smith W V 1954 *Phys. Rev.* **93** 95
For Fe^{2+}, $\zeta = 2S\lambda_{\text{free ion}}$, where $S = 2$ is the total spin.